

---

# Reflectance confocal microscopy



## Diagnostic criteria of common benign and malignant neoplasms, dermoscopic and histopathologic correlates of key confocal criteria, and diagnostic algorithms

Neda Shahriari, MD,<sup>a</sup> Jane M. Grant-Kels, MD,<sup>a,b</sup> Harold Rabinovitz, MD,<sup>c,d</sup> Margaret Oliviero, NP,<sup>c</sup> and Alon Scope, MD<sup>e,f</sup>  
*Farmington, Connecticut; Gainesville and Plantation, Florida; Augusta, Georgia; Tel Aviv, Israel; and New York, New York*

### Learning objectives

After completing this learning activity, participants should be able to identify key criteria for diagnosis of common skin cancers – melanoma, basal cell carcinoma, and squamous cell carcinoma, and distinguish them from common benign lesions – nevi, solar lentigo, seborrheic keratosis, and solar keratosis; recognize RCM correlates of dermoscopic structures of skin lesions and how that enhances the accuracy of dermoscopic diagnosis. Notably, while these benign and malignant skin neoplasms may be challenging to differentiate based on clinical and dermoscopic examination alone, they may be straightforward for RCM diagnosis; and identify histopathological correlates of RCM findings for the common skin neoplasms listed above.

### Disclosures

Dr Rabinowitz is a speaker for Caliber and has received equipment in the past. Ms Oliviero is a speaker and consultant for Caliber ID. Drs Shahriari, Grant-Kels, and Scope have no conflicts of interest to declare.

### Editors

The editors involved with this CME activity and all content validation/peer reviewers of the journal-based CME activity have reported no relevant financial relationships with commercial interest(s).

### Authors

The authors involved with this journal-based CME activity have reported no relevant financial relationships with commercial interest(s).

### Planners

The planners involved with this journal-based CME activity have reported no relevant financial relationships with commercial interest(s). The editorial and education staff involved with this journal-based CME activity have reported no relevant financial relationships with commercial interest(s).

Reflectance confocal microscopy (RCM) is a high-resolution, noninvasive tool that is currently approved by the US Food and Drug Administration for obtaining and interpreting images of the skin and cutaneous neoplasms with the goal of decreasing unnecessary biopsy procedures in patients with benign lesions. The second article in this continuing medical education series focuses on identifying key criteria for the diagnosis of common skin cancers—melanoma, basal cell carcinoma, and squamous cell carcinoma. We contrast these findings with RCM features of common benign lesions—melanocytic nevi, solar lentigo, seborrheic keratosis, lichen planus—like keratosis, and sebaceous hyperplasia. We also correlate the dermoscopic and histopathologic findings with the RCM features. (*J Am Acad Dermatol* 2021;84:17-31.)

---

From the Department of Dermatology,<sup>a</sup> University of Connecticut Health Center, Farmington; Department of Dermatology,<sup>b</sup> University of Florida, Gainesville; Skin and Cancer Associates,<sup>c</sup> Plantation; Dermatology Department,<sup>d</sup> Medical College of Georgia at Augusta University, Augusta; The Kittner Skin Cancer Screening and Research Institute,<sup>e</sup> Sheba Medical Center and Sackler Faculty of Medicine, Tel Aviv University; and the Dermatology Service,<sup>f</sup> Memorial Sloan-Kettering Center, New York.

Supported by the Israel Science Foundation (ISF-1546-16).

Dr Rabinowitz is a speaker for Caliber and has received equipment in the past. Ms Oliviero is a speaker and consultant for Caliber ID. Drs Shahriari, Grant-Kels, and Scope have no conflicts of interest to declare.

Accepted for publication May 14, 2020.

Reprint requests: Neda Shahriari, MD, Department of Dermatology, University of Connecticut Health Center, 21 South Rd, Farmington, CT 06032. E-mail: [shahriari@uchc.edu](mailto:shahriari@uchc.edu).

0190-9622/\$36.00

---

© 2020 by the American Academy of Dermatology, Inc.

<https://doi.org/10.1016/j.jaad.2020.05.154>

**Date of release: January 2021.**

**Expiration date: January 2024.**



Scanning this QR code will direct you to the CME quiz in the American Academy of Dermatology's (AAD) online learning center where after taking the quiz and successfully passing it, you may claim 1 AMA PRA Category 1 credit. NOTE: You must have an AAD account and be signed in on your device in order to be directed to the CME quiz. If you do not have an AAD account, you will need to create one. To create an AAD account: go to the AAD's website: [www.aad.org](http://www.aad.org).

**Key words:** BCC; benign neoplasms; diagnostic algorithms; melanoma; nevi; reflectance confocal microscopy; SCC.

Reflectance confocal microscopy (RCM) is currently being used as an adjunct to clinical and dermoscopic evaluation of cutaneous neoplasms. In the first article in this continuing medical education series, we described the applications of RCM as a noninvasive tool to decrease unnecessary biopsy procedures by increasing diagnostic specificity and sensitivity in different clinical contexts. Given the relative gap in knowledge of RCM image interpretation, the focus of the second article in this series is to present the primary RCM characteristics and algorithms of benign and malignant cutaneous neoplasms and provide dermoscopic and histopathologic correlations.

## BENIGN NONMELANOCYTIC LESIONS

### Solar lentigo

Clinically, solar lentigo appears as a brown to tan macule or patch in actinically damaged skin. It is sometimes challenging to distinguish from lentigo maligna and pigmented Bowen's disease, prompting frequent biopsy procedures.<sup>1</sup> With RCM, solar lentigo displays a regular honeycomb pattern of the spinous-granular layers.<sup>2-4</sup> The regular honeycomb pattern correlates to a lack of keratinocytic atypia on histopathology. Solar lentigo on RCM is distinct at the level of the dermoepidermal junction (DEJ), demonstrating an increased density of "edged papillae"—dermal papillae rimmed by bright uniform basal cells.<sup>2</sup> This refractile layer of cells correlates with a cross-sectional view of rete ridges that are lined by pigmented basal keratinocytes.<sup>2</sup> Variability in the shape of the dermal papillae can be noted—ovoid, annular, and polycyclic.<sup>2</sup> Bright elongated cords with bulbous tips can also be visualized at the DEJ, corresponding with elongated pigmented rete ridges ("dirty feet") visualized by histopathology (Fig 1).<sup>3</sup> The shape of dermal papillae is dependent on the degree of budding and complexity of anastomosis between the elongated retes. The edged papillae and cord-like rete ridges correlate with fingerprinting and the reticular pattern seen with dermoscopy, respectively.<sup>5</sup> Table I summarizes the key RCM features of solar lentigo.

### Seborrheic keratosis

Seborrheic keratoses (SKs) are pink to brown stuck-on waxy papules, plaques, or nodules. Dermoscopy highlights the cerebriform epidermal architecture as well as milia-like cysts and comedo-like openings.<sup>6</sup> Irritation, trauma, and regression can

cause changes within an SK that make it clinically challenging to distinguish from skin cancer.<sup>7-9</sup>

With RCM, SKs show epidermal surface projections, correlating with the clinical and dermoscopic cerebriform surface.<sup>10-12</sup> In addition, keratin-filled surface invaginations or corneal plugs, which are round to linear depressions that harbor structureless amorphous refractile keratin debris by RCM, correlate with comedo-like openings on dermoscopy.<sup>5,11</sup> At varying epidermal levels, corneal pseudocysts can be observed as white round structures that are highly refractile because of their keratin content.<sup>11</sup> These structures correlate with milia-like cysts on dermoscopy.<sup>13</sup> The regular honeycomb pattern of the spinous-granular layer is preserved in nonpigmented SK, while a regular cobblestone pattern can be visualized in pigmented SKs.<sup>11</sup> Epidermal acanthosis can be seen on RCM as a broadened honeycomb pattern, whereby the keratinocytes appear regularly arranged, yet the polygonal outlines of the honeycomb are thicker and brighter than usual.<sup>14</sup> At the level of the DEJ, densely packed oval to polymorphous dermal papillae, often with a ring pattern, are observed. Furthermore, elongated bright tubular structures with bulbous projections, correlating with the thick fingerprint-like structures with dermoscopy, can be seen at this level (Fig 2).<sup>5,10,11</sup> SKs have an RCM vascular pattern of dilated looped vessels, correlating with hairpin vessels with dermoscopy.<sup>11</sup> Table II summarizes the key RCM features of SKs.

### Lichen planus–like keratosis

Lichen planus–like keratosis is a macule or thin papule occurring on sun-damaged skin and is thought to be a solar lentigo or SK undergoing inflammation and regression.<sup>15,16</sup> With RCM, similar to an SK, corneal plugs or pseudocysts can be observed.<sup>14</sup> Given the benign nature of this lesion, the regular honeycomb pattern is preserved in the spinous-granular layers in the majority of lesions with an occasional broadened honeycomb pattern if the epidermis is acanthotic.<sup>14</sup> At the DEJ, foci with elongated cords with bulbous tips can be observed suggestive of residual features of SK or solar lentigo.<sup>14</sup> Most prominently, at the level of the papillary dermis, a dense infiltrate of bright dots and plump-bright cells can be seen, representing the band-like lymphocytic infiltrate and melanophages on histopathology, respectively (Fig 3). The correlative dermoscopic feature is gray-dot granularity.<sup>14</sup>

*Abbreviations used:*

AK:	actinic keratosis
BCC:	basal cell carcinoma
DEJ:	dermoepidermal junction
DN:	dysplastic nevus
LM:	lentigo maligna
LMM:	lentigo maligna melanoma
LPLK:	lichen planus–like keratosis
RCM:	reflectance confocal microscopy
SCC:	squamous cell carcinoma
SK:	seborrheic keratosis

In foci with flattening of the DEJ, there is an abrupt transition from the epidermis to dermis, without visible dermal papillae. Highly refractile bundles at the papillary dermis correlate with fibrosis, while curled and clumped bright fibers correlate with solar elastosis.<sup>14</sup> Table III shows the key RCM findings of lichen planus–like keratosis.

### Sebaceous hyperplasia

Sebaceous hyperplasia appears as a yellow soft umbilicated papule with serpentine radial vessels (“crown vessels”), making it occasionally difficult to distinguish from basal cell carcinoma (BCC).<sup>17,18</sup> Compared with BCC, however, the blood vessels in sebaceous hyperplasia lack branching and do not cross the center of the lesion. With RCM, sebaceous hyperplasia is characterized by a dilated central follicular infundibulum containing sebum and keratin debris, correlating with the central umbilication noted clinically and dermoscopically.<sup>19,20</sup> Surrounding the central umbilication, sebaceous lobules are composed of round cells with dark nuclei and refractile speckled cytoplasm—these have been described as “morula-shaped” (ie, reminiscent of morula stage of embryogenesis; Fig 4).<sup>19,21–23</sup> In the papillary dermis, dark tubular vessels can be observed running parallel to the plane of RCM,<sup>19</sup> correlating with crown vessels on dermoscopy. Sebaceous hyperplasia usually demonstrates solar elastosis in the dermis, in contrast with the fibroplasia that is often seen in BCC.<sup>20</sup> Table IV provides a summary of key RCM features of sebaceous hyperplasia.

## MALIGNANT NONMELANOCYTIC LESIONS

### BCC

As the most common skin cancer,<sup>24</sup> BCC has different histopathologic subtypes, including superficial, nodular, and morpheiform. At the level of the spinous layer with RCM, keratinocytes may display a regular honeycomb or appear as elongated along an axis, a pattern denoted as “streaming”; this feature can be observed when the basaloid tumor

aggregates push against and compress the epidermis.<sup>25</sup> The basaloid tumor aggregates may appear on RCM as either “bright tumor cords/islands”—high refractility aggregates caused by increased melanin— or “dark silhouettes”—low refractility aggregates that are darker than the surrounding stroma (Fig 5).<sup>26</sup>

The bright tumor islands are frequently seen in pigmented BCCs. They show peripheral palisading of nuclei and are often delineated by dark clefting, representing low-refractility mucin and stromal retraction.<sup>25</sup> Dendritic cells can be observed within tumor islands representing melanocytes.<sup>27</sup> The bright tumor islands that contain melanin correlate with the blue ovoid nests and blue globules observed with dermoscopy.<sup>28</sup> Melanophages, appearing as plump-bright cells in the papillary dermis, can also be seen in pigmented BCCs.<sup>29</sup> The dermoscopic correlate is gray-dot granules.<sup>28</sup> The dark silhouettes can be visualized in nonpigmented BCCs and particularly in superficial BCC.<sup>29</sup> Within the tumor islands, the neoplastic cells may be oriented along the same axis, known as “nuclear polarization.”<sup>25,26</sup> In the stroma that interweaves between tumor islands, highly refractile collagen bundles can be observed, correlating with dermal fibrosis surrounding the basaloid aggregates on histopathology. Tortuous canalicular blood vessels, running parallel to the plane of RCM imaging, can be seen within the stroma and correlate to the in-focus branched (arborizing) dilated vessels characteristic with dermoscopy<sup>29</sup>; the histopathologic correlate is cross-sectional vessels between the dermal tumor nodules.<sup>28</sup> Table V provides key RCM findings in BCC.

### Actinic keratosis

Actinic keratoses (AKs) appear as scaly erythematous macules or flat papules; histologically they are characterized by partial thickness keratinocytic atypia involving the lower half of the epidermis and the basal layer. At the surface of the skin, RCM shows parakeratosis—the presence of bright round keratinocytes with retained nuclei in the stratum corneum, and hyperkeratosis—increased brightness, surface irregularity, and thickening of the stratum corneum of  $>20 \mu\text{m}$  (that could be measured by counting stack images from the top of the stratum corneum to the granular layer); those features correlate with the alternating para- and orthokeratosis seen with histopathology and with the evident scale by dermoscopy.<sup>30–33</sup> If a stack of RCM optical sections is obtained from the stratum corneum to the basal layer, there is a difference in the honeycomb pattern between the upper epidermis that shows a regular

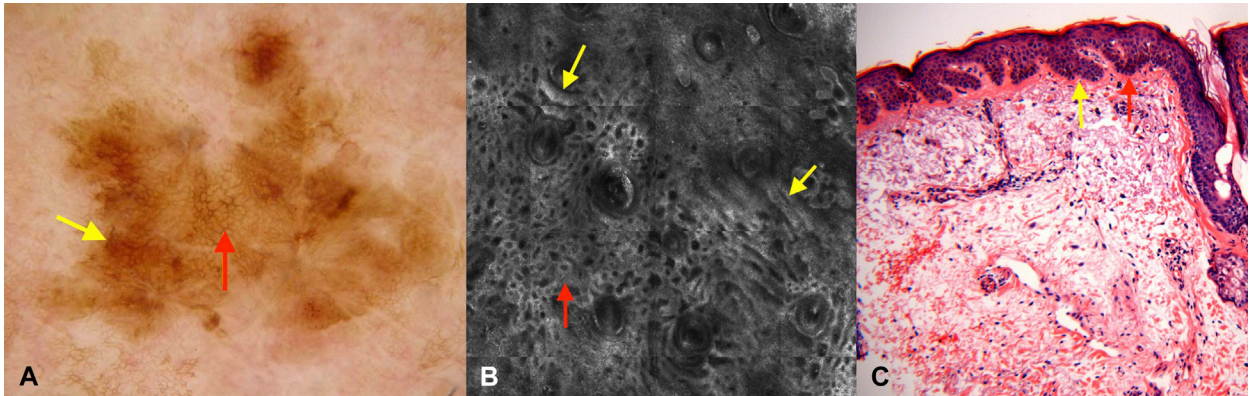


**Fig 1.** Solar lentigo. **A**, Dermoscopy demonstrating a brown macule with moth-eaten borders and pigmented lines in parallel (yellow arrow) and network-like formation (red arrow). **B**, Reflectance confocal microscopy mosaic ( $1.5 \times 1.5 \text{ mm}^2$ ) at the level of the dermoepidermal junction shows bright cords that are laid out in parallel (yellow arrows) or intersecting fashion (red arrow), correlating with the dermoscopic network-like structures. **C**, Photomicrograph demonstrating epidermal hyperplasia and elongated pigmented rete (“dirty feet”; yellow arrow) showing fusion of adjacent retes (red arrow). The elongated pigmented retes correlate with the elongated bright cords on reflectance confocal microscopy. (C, Hematoxylin–eosin stain; original magnification:  $\times 100$ .)

**Table I.** Summary of major reflectance confocal microscopy features of solar lentigo

Regular honeycomb pattern in the spinous-granular layers
Increased number of dermal papillae with varying shapes—ovoid, annular, cerebriform, and polycyclic at the dermoepidermal junction
Ring pattern of bright keratinocytes around dermal papillae (edged papillae)
Elongated bright cords with bulbous projections at the dermoepidermal junction

honeycomb and the lower epidermis, which displays an irregular honeycomb, indicating a loss of normal epidermal stratification.<sup>33</sup> The irregular honeycomb pattern can be visualized with RCM as bright cellular outlines of keratinocytes varying in size and shape and in the thickness and brightness of the lines varying in size, outline, and refractility, mostly in the lower portions of the epidermis.<sup>30</sup> In AKs, the infundibular epithelium is usually “spared” and retains a regular honeycomb pattern. The basal layer of the epidermis may show bulbous extensions into the dermis with RCM, correlating with budding of the basal layer into the dermis on histopathology. In the papillary dermis, a stroma with bright curled fibers can be visualized, correlating to solar elastosis, as well as increased blood flow and inflammation, appearing as bright dots on RCM.<sup>29</sup>

### Squamous cell carcinoma

Squamous cell carcinoma (SCC) presents as a hyperkeratotic papule, nodule, or plaque most commonly on sun-damaged skin. Clinically it can mimic hypertrophic AKs and inflamed SKs. With RCM, SCC shows at the corneal layer confluent and irregular hyperkeratosis or parakeratosis.<sup>34,35</sup> A markedly thickened scale can obscure RCM imaging of the underlying epidermis, and in these cases, imaging should concentrate on the periphery of the neoplasm. The regular honeycomb pattern is lost in the spinous-granular layers and instead there is “keratinocyte disarray”—an irregular honeycomb or disarranged epidermal pattern can be seen (Fig 6), correlating on histopathology with full-thickness keratinocytic atypia.<sup>34,35</sup> In contrast with AK, there are no “spared islands” of regular honeycomb, and the keratinocytic disarray is confluent. Bright round atypical cells can occasionally be observed within the spinous layer, representing dyskeratotic cells.<sup>20</sup> At the DEJ, dermal papillae harboring tortuous blood vessels running perpendicular to the plane of imaging can be seen with RCM.<sup>34,35</sup> This RCM vascular pattern has been previously described as the “buttonhole sign”<sup>36</sup> and corresponds to dermoscopic glomerular (coiled) or dotted vessels.<sup>28,29</sup>

Because of the depth limitations and the horizontal orientation of imaging of RCM, distinguishing SCC in situ from invasive SCC may be challenging. Invasive SCC with RCM can show in the papillary

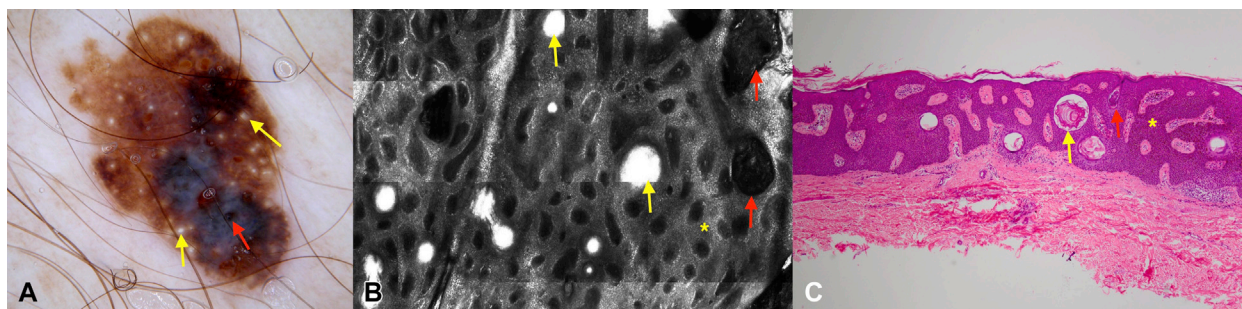


**Fig 2.** Seborrheic keratosis. **A**, Dermoscopy shows a sharply-demarcated papule with milium-like cysts (yellow arrows) and comedo-like openings (red arrows), as well as irregular pigmentation including a blue-white focus. **B**, Reflectance confocal microscopy mosaic ( $1.75 \times 1.5 \text{ mm}^2$ ) at the level of the dermoepidermal junction demonstrates bright horn pseudocysts (yellow arrows), keratin-filled invaginations (red arrows), and thick interweaving anastomosing cords with a regular cobblestone pattern of keratinocytes (asterisk). **C**, Photomicrograph demonstrating an acanthotic epidermis with a reticulated pattern that correlates with the elongated and anastomosing rete on reflectance confocal microscopy (asterisk). The pigmented keratinocytes account for the reflectance confocal microscopy cobblestone pattern. There are also horn pseudocysts (yellow arrows) and keratin-filled invaginations (red arrows). (C, Hematoxylin–eosin stain; original magnification:  $\times 40$ .)

**Table II.** Summary of major reflectance confocal microscopy features of seborrheic keratosis

Papillated epidermal hyperplasia
Keratin-filled invaginations and horn pseudocysts
Regular or broadened honeycomb pattern or cobblestone pattern of the spinous-granular layers
Densely packed round to polymorphous edged dermal papillae
Interconnecting bright cords with bulbous projections at the dermoepidermal junction

dermis tumor aggregates—seen as cellular aggregates with irregular and discohesive margins, as well as speckled nucleated cells (roundish to polygonal cells with speckled appearance and a dark nucleus), which have a polygonal shape that differentiate them from melanophages.<sup>37</sup> In addition, with RCM invasive SCC more frequently shows ulceration or surface erosion and less frequently surface hyperkeratosis and the buttonhole sign than in situ SCC.<sup>37</sup>

RCM of pigmented SCC in situ shows an atypical honeycomb with nonconfluent spindle-shaped cells with delicate dendritic branches infiltrating the suprabasal epidermis, correlating with Langerhans cells. In addition, there are multiple bright DEJ edged papillae that are small and roundish in shape and with widened interpapillary spaces, mostly at the lesion's periphery.<sup>38</sup> Table VI provides key RCM findings in SCC.

## BENIGN MELANOCYTIC NEVI

### Common nevi

RCM can help in the discernment of so-called common nevi from melanoma. To understand the RCM features of nevi we need to classify nevi in accordance with the degree of melanocytic proliferation (single cells or in aggregate) and architecture (junctional, compound, or dermal). Clinically, junctional nevi appear as uniform round brown macules that are symmetric with regular borders. Compound nevi present as papules, but similarly appear round to oval and brown to tan; dermal nevi may be pink to light brown and demonstrate a more exophytic silhouette.<sup>39</sup>

With RCM, junctional nevi demonstrate preservation of the regular honeycomb and cobblestone patterns of the epidermis.<sup>39</sup> Pagetoid cells are not observed within the epidermis, though slender dendritic cells representing Langerhans cells may be seen in an inflamed nevus.<sup>40</sup> At the DEJ, 2 RCM patterns may be observed: ring pattern or meshwork pattern (Fig 7).<sup>41</sup> The ringed architecture shows edged papillae, characterized by dark dermal papillae surrounded by a ring-like rim of bright cells, representing pigmented basal keratinocytes and small melanocytes.<sup>39,40,42-44</sup> The dermoscopic correlate is the pigment network.<sup>40</sup> Histopathologically, these features correspond to a nevus with a mostly lentiginous component at the DEJ.<sup>45</sup> The meshwork pattern with RCM shows thickened, interconnecting, bright, elongated aggregates that widen the interpapillary spaces (ie, the rete ridges); the meshwork correlates with elongated junctional nests

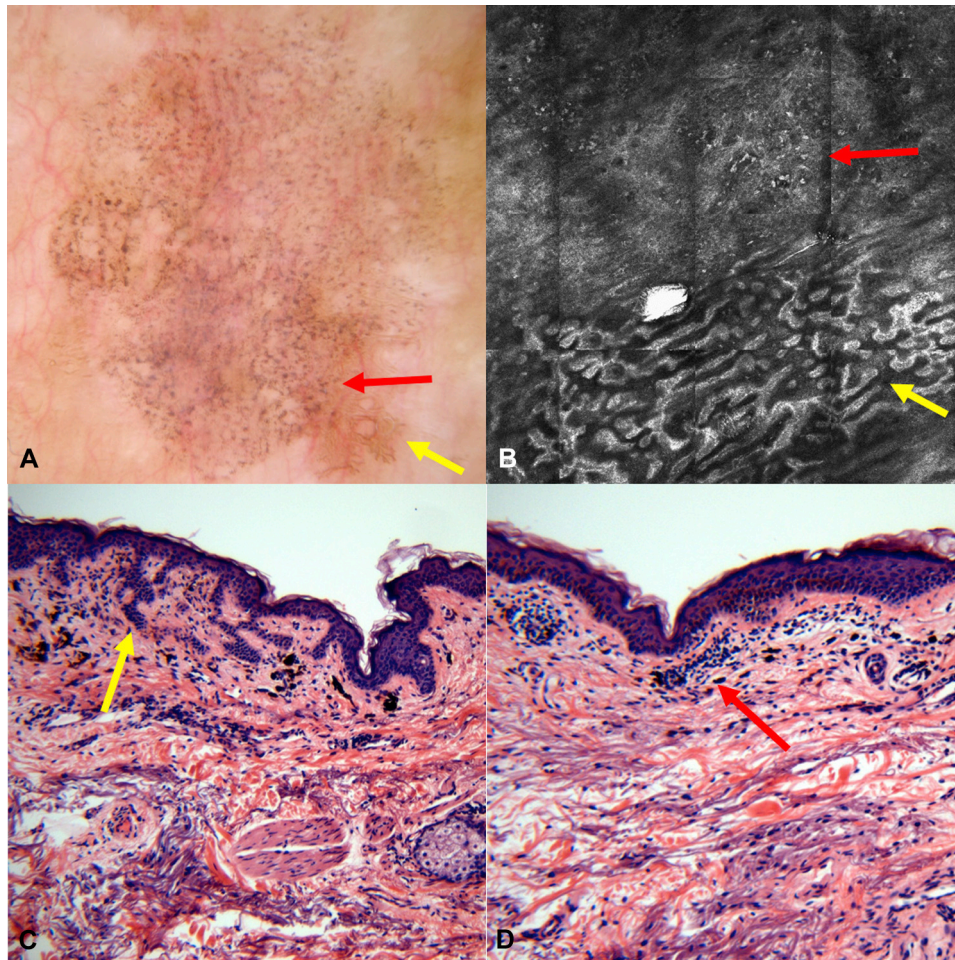


**Fig 3.** Lichen planus–like keratosis. **A**, Dermoscopy shows a poorly defined macule with diffuse granularity (red arrow). A moth-eaten border can be appreciated alongside fingerprint-like areas (yellow arrow). **B**, Reflectance confocal microscopy mosaic ( $1.5 \times 1.5 \text{ mm}^2$ ) at the level of the dermoepidermal junction demonstrates elongated cords with bulbous projections, correlating with elongated rete (yellow arrow). Bright dots and plump-bright cells (red arrow), correspond to dense inflammatory cells, composed of lymphocytes and macrophages, respectively. **C** and **D**, Photomicrograph depicting foci with elongated retes (yellow arrow) and other areas with a flattened dermoepidermal junction and an inflammatory infiltrate composed of lymphocytes and melanophages (red arrow). (**C** and **D**, Hematoxylin–eosin stain; original magnification:  $\times 100$ .)

**Table III.** Summary of major reflectance confocal microscopy features of lichen planus–like keratosis

Regular honeycomb pattern of the spinous granular layers
Foci with elongated bright cords with bulbous projections at the dermoepidermal junction
Other foci with abrupt transition between the epidermis and dermis (flattening of the dermoepidermal junction)
Numerous bright dots and plump-bright cells (melanophages) at the papillary dermis

of melanocytes along the sides and tips of the rete ridges, with bridging of adjacent retes on histopathology. Dense bright round structures bulging into the papillae, corresponding to discrete junctional nests, can also be seen.<sup>40,45</sup> The dermoscopic equivalent may be seen as thicker reticular or reticular-globular pattern.<sup>40</sup>

Compound and dermal nevi also show preservation of the normal honeycomb pattern with RCM. The dermal component is visualized as discrete nests

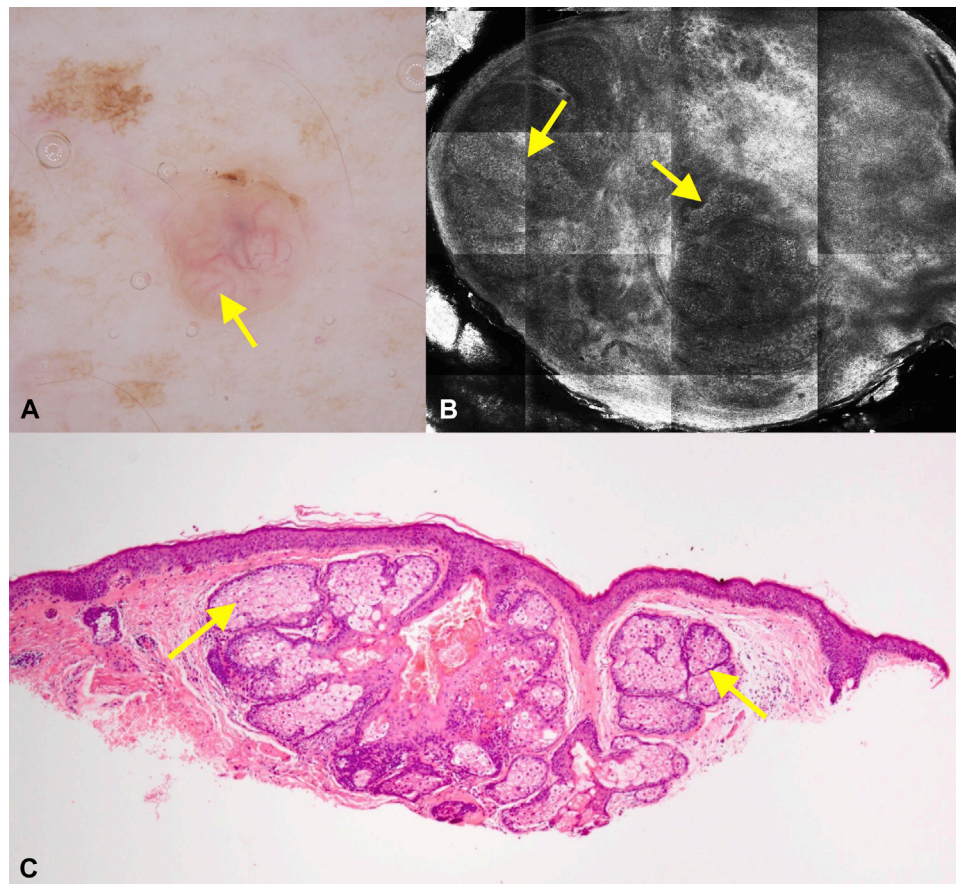


**Fig 4.** Sebaceous hyperplasia. **A**, Dermoscopy of a papule with crown vessels and yellow-white lobular structures (arrow) **B**, Reflectance confocal microscopy mosaic ( $1.8 \times 1.8 \text{ mm}^2$ ) at the level of papillary dermis demonstrates a lobulated proliferation composed of round cells with bright speckled cytoplasm and a centrally located nucleus representing sebocytes (arrows). **C**, Photomicrograph shows a dilated infundibulum with surrounding large sebaceous lobules (arrows). (**C**, Hematoxylin–eosin stain; original magnification:  $\times 40$ .)

**Table IV.** Summary of major reflectance confocal microscopy features of sebaceous hyperplasia

Dilated central follicular infundibulum
Morulae-shaped sebaceous lobules composed of round cells with speckled cytoplasm and dark nuclei
Dark tubular blood vessels

that fill and often expand the dermal papillae, termed clod-pattern (Fig 8), which correlates with a globular dermoscopic pattern.<sup>40,46</sup> The refractivity of the nests varies and is low in nonpigmented nevi. In a compound nevus, the dermal nests would be associated with a meshwork pattern at the DEJ.<sup>41</sup> A summary of key RCM features of common nevi is shown in Table VII.

#### Dysplastic (atypical) nevi

Dysplastic nevi (DN) may be difficult to distinguish from melanoma with RCM. Clinically, DN appear as brown macules with irregular pigmentation and often a central papular component. Similar to dermoscopy and histopathology, RCM features of DN are on a spectrum between common nevi and melanomas.<sup>47,48</sup> For DN with mild atypia, a combination of ring and meshwork pattern can be visualized at the DEJ.<sup>49</sup> There may be poor demarcation at the periphery, which correlates on histopathology to the shouldering phenomenon—an epidermal component extending laterally to the dermal component.<sup>49</sup> Melanocytes in pagetoid spread can be rarely detected, but only at the center of the lesion.<sup>49</sup> Junctional nests can be observed, as well as highly refractile collagen fibers (representing fibrosis) and small inflammatory cells and melanophages.<sup>49</sup> If compound, clods will be noted in the papillary dermis centrally.

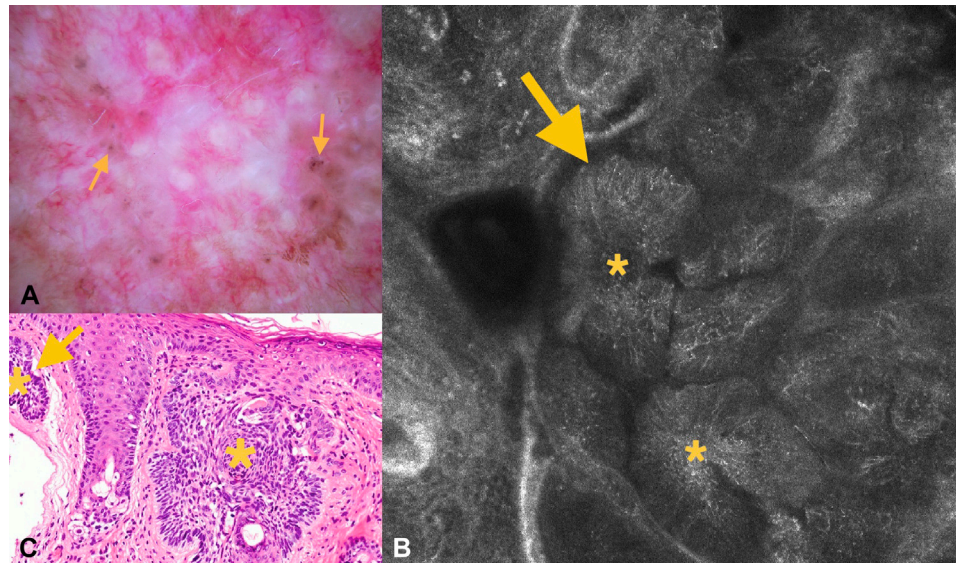


**Fig 5.** Basal cell carcinoma. **A**, Dermoscopy shows a pink-white papule with brown-gray globules and dots (arrows). **B**, Reflectance confocal microscopy optical section ( $0.75 \times 0.75 \text{ mm}^2$ ) shows bright well-demarcated tumor islands (asterisks) with surrounding dark clefting (arrow). **C**, Photomicrograph depicting the corresponding basaloid aggregates (asterisks) with focal retraction from the surrounding fibrotic stroma (arrow). (C, Hematoxylin–eosin stain; original magnification:  $\times 200$ .)

**Table V.** Summary of major reflectance confocal microscopy features of basal cell carcinoma

Regular honeycomb or keratinocytic “streaming” of the epidermis spinous layer
Basaloid tumor aggregates in the dermis appearing as “bright tumor cords/islands” with peripheral palisading or nuclei or as “dark silhouettes”
Dark clefts around tumor aggregates
Fibroplasia with refractile collagen bundles in the dermis
Linear (horizontally oriented) tortuous blood vessels in the dermis

Moderate and severe DN depict more asymmetry. The epidermis typically depicts the honeycomb and cobblestones patterns, but there may be some irregularity.<sup>49</sup> Atypical melanocytes at the DEJ are more widespread but involve  $<50\%$  of the lesion. Pagetoid cells may be observed<sup>49</sup> but involve  $<50\%$  of the lesion and are noted only focally and at the center of the lesion.<sup>50</sup> At the DEJ, a meshwork pattern, with some variability in the thickness and spacing of the interconnecting elongated junctional aggregates, is present centrally and a ring pattern is noted peripherally.<sup>49</sup> Inflammation and fibrosis can be observed. The presence of atypical melanocytes in some DN can make them indistinguishable from melanoma.<sup>49,51</sup> Table VII provides key RCM features of DN.

### Spitz nevi

Spitz nevi can be clinically difficult to distinguish from melanoma. They most commonly have a star-burst or globular pattern under dermoscopy.<sup>52</sup> With RCM, there is preservation of the regular epidermal honeycomb and cobblestone patterns. When the epidermis is acanthotic, a broadened honeycomb may be seen. Pagetoid cells can be observed at the center and are composed of dendritic- or rounded-nucleated cells.<sup>53</sup> The star-burst pattern seen dermoscopically manifests itself as confluent elongated junctional nests or clods at the periphery of the lesion.<sup>53</sup> The papillary dermis usually reveals nests of melanocytes and melanophages. Table VII provides key RCM features of spitz nevi.

### MALIGNANT MELANOMA

With RCM, melanoma is often associated with an irregular honeycomb pattern and irregular cobblestone pattern because of the atypical melanocytes infiltrating the epidermis.<sup>20,29</sup> Pagetoid spread of atypical melanocytes appears as refractile round or dendritic nucleated cells (Fig 9).<sup>50</sup> Melanocytes may appear singly or in small clusters. At the level of the DEJ, nonedged dermal papillae are characteristic, appearing in varying sizes alongside widened interpapillary spaces caused by infiltration of atypical melanocytes. The overall pattern is disorganized/chaotic—a ringed, meshwork, or clod pattern that is asymmetric or irregular in



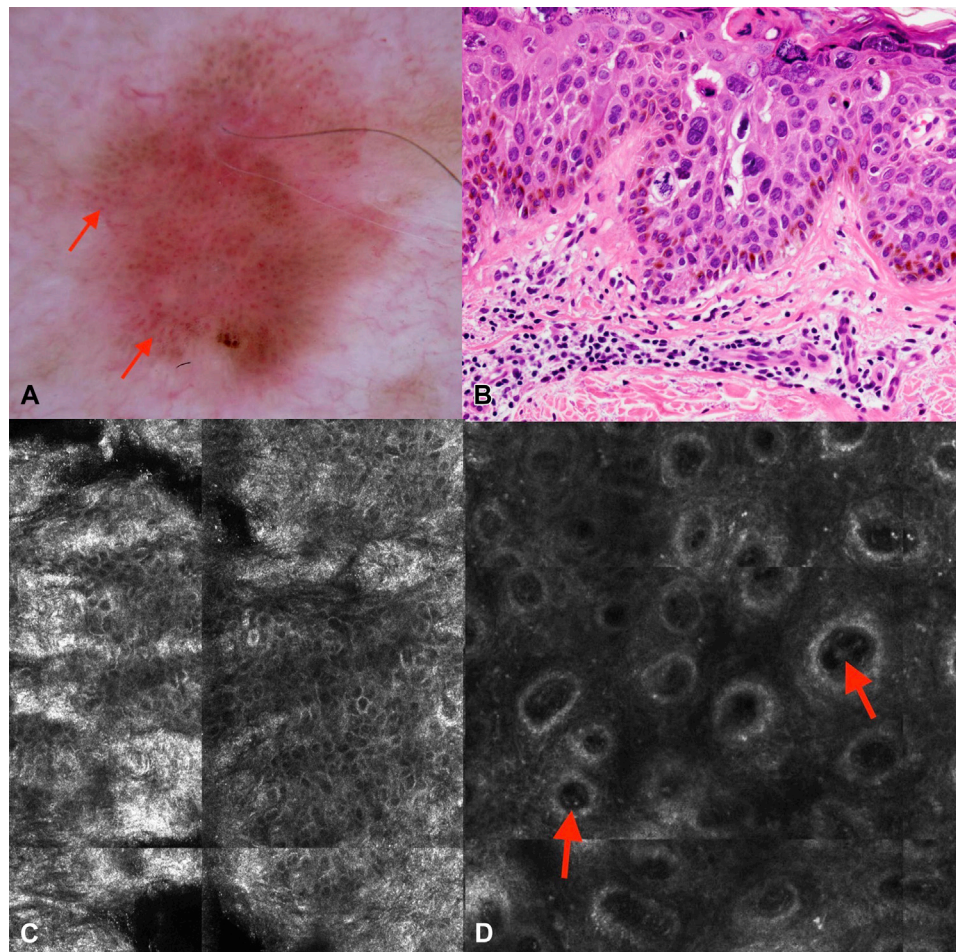


**Fig 6.** Pigmented squamous cell carcinoma in situ. **A**, Dermoscopy shows a brown-pink macule with dotted vessels (arrows). **B**, Photomicrograph demonstrates full-thickness keratinocytic atypia. **C**, Reflectance confocal microscopy ( $0.75 \times 1.0 \text{ mm}^2$ ) at the level of the spinous-granular layers shows irregularity of size and shapes of keratinocytes forming an irregular (atypical) honeycomb pattern that correlates with the keratinocytic atypia. **D**, Reflectance confocal microscopy mosaic ( $2 \times 2 \text{ mm}^2$ ) at the level of the dermoepidermal junction shows edged papillae. Blood vessels in the papillae display the “buttonhole sign” (arrows), correlating with the dotted vessels seen with dermoscopy. (**B**, Hematoxylin–eosin stain; original magnification:  $\times 200$ .)

**Table VI.** Summary of major reflectance confocal microscopy features of squamous cell carcinoma

Irregular surface with hyperkeratosis or parakeratosis
Keratinocyte disarray—an irregular honeycomb or disarranged epidermal pattern in the spinous-granular layers
Dyskeratotic cells
“Buttonhole sign” in the dermal papilla representing coiled, vertically oriented blood vessels
Edged papillae at the dermoepidermal junction and focal dendritic cells (Langerhans cells) at the epidermis spinous layer in pigmented squamous cell carcinoma

appearance.<sup>54</sup> Loss of DEJ pattern is mostly caused by flattening of the DEJ or to infiltration by dense sheets of melanocytes. Junctional thickening and an atypical meshwork pattern (Fig 9) may be observed in both melanoma and some DN. In melanoma, however, the junctional thickening that causes the atypical meshwork pattern markedly varies in thickness and refractility, while nevi display greater regularity.<sup>29</sup> The irregular meshwork correlates with an atypical pigment network with dermoscopy.<sup>55</sup> The findings described here are characteristic of most melanomas that arise on the trunk and extremities (superficial spreading

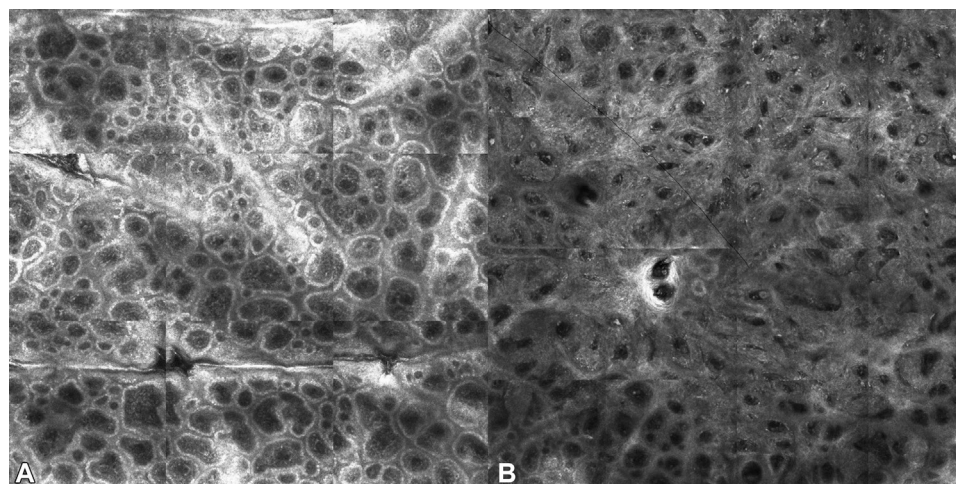


**Fig 7.** Melanocytic nevus. Reflectance confocal microscopy mosaics at the level of the dermoepidermal junction showing a regular architecture composed of (A) ringed and (B) meshwork patterns.

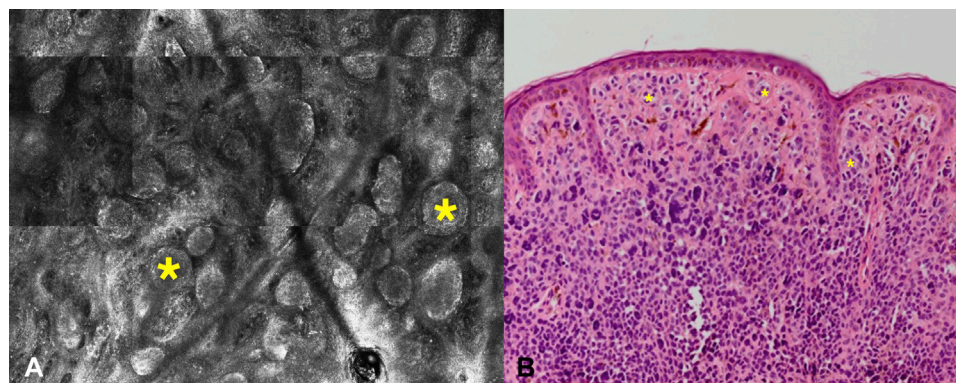


**Fig 8.** Melanocytic nevus. **A**, Reflectance confocal microscopy mosaic ( $1.0 \times 1.25 \text{ mm}^2$ ) at the level of the dermoepidermal junction demonstrates a regular clod pattern composed of junctional and dermal nests (asterisks). **B**, Photomicrograph shows nests of melanocytes (asterisks) at the DEJ and dermis. (**B**, Hematoxylin–eosin stain; original magnification:  $\times 200$ .)

**Table VII.** Summary of major reflectance confocal microscopy features of nevi

Common nevi	Dysplastic nevi	Spitz nevi
Regular honeycomb or cobblestone pattern in the epidermis	Regular to mildly irregular honeycomb or cobblestone pattern of epidermis	Regular or broadened honeycomb or cobblestone pattern in the epidermis
Regular DEJ pattern: ring, meshwork, or clod patterns depending on nevus type (junctional, compound, or dermal)	Mild to marked distortion of DEJ architecture at the center of the lesion Epidermal component extending laterally to the dermal component Cells in pagetoid spread may be focally present at the center of the lesion	Pagetoid infiltration in the center of the lesion Confluent elongated junctional clods at the periphery Disarrangement of DEJ with nonedged papillae and numerous junctional nests

DEJ, Dermoepidermal junction.

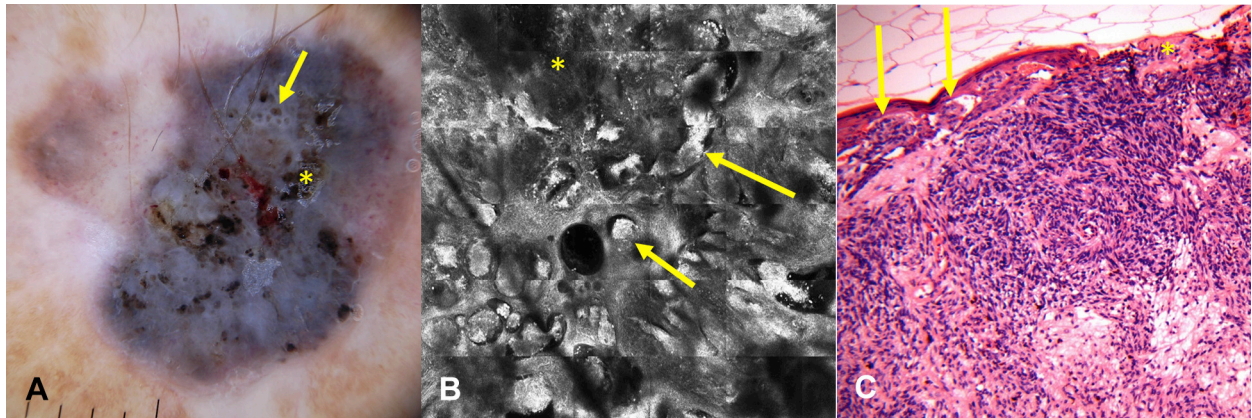


**Fig 9.** Invasive melanoma. **A**, Dermoscopy shows a blue-black ulcerated (asterisk) papule with blue-white veil, polymorphous vessels, and brown globules/dots (yellow arrows). **B**, Reflectance confocal microscopy mosaic ( $2.5 \times 2.5 \text{ mm}^2$ ) at the level of the dermoepidermal junction shows an irregular clod pattern with bizarre-shaped and unevenly spaced nests of atypical melanocytes (arrows). **C**, Photomicrograph demonstrating poorly aggregated melanocytic nests that are irregularly shaped and spaced (arrows). Focal area of ulceration is noted (asterisk). (**C**, Hematoxylin–eosin stain; original magnification:  $\times 200$ .)

**Table VIII.** Summary of major reflectance confocal microscopy features of melanoma

Atypical cells in pagetoid spread. The suspicion increases when cells are round-nucleated, reaching high in the suprabasal epidermis or diffusely infiltrating the lesion
Atypical cells at the DEJ—large ( $>20 \mu\text{m}$ ), round or dendritic nucleated cells, either presenting as solitary units or forming clusters. The suspicion for melanoma increases with a cellular density $>5/\text{mm}^2$ or with cellular pleomorphism
DEJ disarray—disorganized pattern (ring, meshwork, or clod patterns that are asymmetrically distributed or irregular in appearance) or the presence of nonedged papillae
Loss of DEJ pattern—areas that lack any of the recognizable DEJ patterns (ring, meshwork, and clod patterns)
In lentigo maligna—sheets of atypical melanocytes, mostly with a dendritic shape, in the basal epidermis, surrounding and extending down adnexal openings
In nodular melanoma—cerebriform dermal nests
In amelanotic melanoma—“hyporeflective” pagetoid cells in the suprabasal epidermis

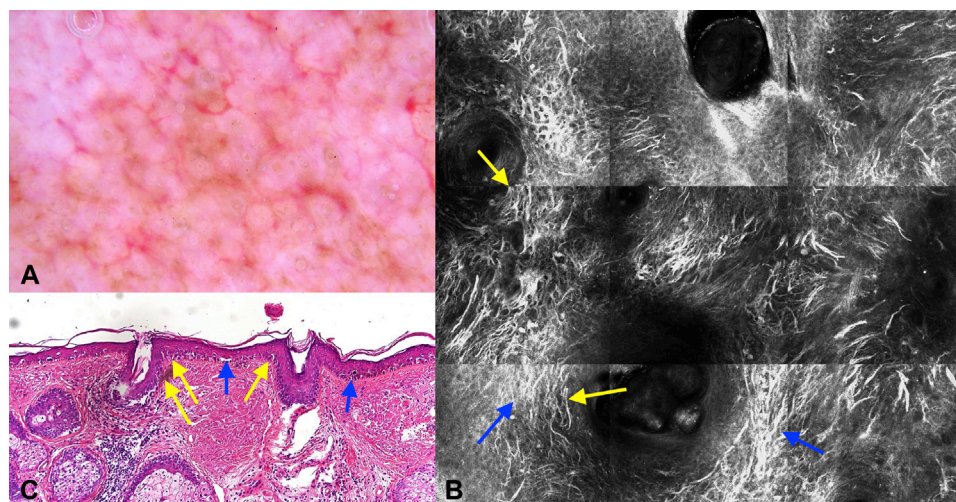


**Fig 10.** Lentigo maligna. **A**, Dermoscopy shows a poorly defined brown patch with an annular pattern and asymmetric follicular openings. **B**, Reflectance confocal microscopy mosaic ( $1.5 \times 1.5 \text{ mm}^2$ ) at the level of basal and spinous epidermis shows dendritic atypical melanocytes in sheets (blue arrows), further extending into adnexal structures (yellow arrows). **C**, Photomicrograph demonstrating proliferation of atypical melanocytes along the basal layer (blue arrows), as well as pagetoid infiltration at the suprabasal epidermis and extension down adnexal structures (yellow arrows). (**C**, Hematoxylin–eosin stain; original magnification:  $\times 100$ .)

**Table IX.** Summary of major reflectance confocal microscopy algorithms for melanoma diagnosis

RCM method	Methodology
Pellacani RCM score <sup>42</sup>	RCM score ranges from 0-8 points Major criteria (2 points each): nonedged papillae at basal layer and cytologic atypia (mild or marked) Minor criteria (1 point each): roundish cells spreading in pagetoid fashion, pagetoid cells widespread throughout lesion, cerebriform clusters in papillary dermis, or nucleated cells within dermal papilla Score $\geq 3$ essential for melanoma diagnosis
Segura 2-step method <sup>63</sup>	Two steps: 1. Is lesion melanocytic tumor or not? Evaluate following criteria: <ul style="list-style-type: none"> <li>• Cobblestone pattern (C)</li> <li>• pagetoid infiltration (P)</li> <li>• Dermal nests (N)</li> <li>• Widespread dermal papilla (DP)</li> </ul> CPN <sup>-</sup> /DP <sup>-</sup> : Nonmelanocytic lesion if fulfills RCM features of BCC, SK, DF, or vascular lesion. If not, consider melanoma CPN <sup>-</sup> /DP <sup>+</sup> : Melanocytic lesion or nonmelanocytic. Evaluate for RCM features of BCC, SK, DF, or vascular lesion. If not, consider melanoma CPN <sup>+</sup> /DP <sup>-</sup> : Melanocytic lesion CPN <sup>+</sup> /DP <sup>+</sup> : Melanocytic lesion 2. If lesion determined to be melanocytic, evaluate for features of melanoma vs nevus: Protective features (suggestive of nevi): <ul style="list-style-type: none"> <li>• Typical basal cells (-1 score)</li> <li>• Edged papilla (-1 score)</li> </ul> Risk features (suggestive of melanoma) <ul style="list-style-type: none"> <li>• Roundish pagetoid cells (+1 score)</li> <li>• Atypical nucleated dermal cells (+1 score)</li> </ul> -2: Most probable nevus -1: Probable nevus, may be melanoma 0-2: Most probable melanoma
Langley method <sup>66</sup>	Morphologic criteria used for melanoma diagnosis <ul style="list-style-type: none"> <li>• Epidermal disarray with loss of the normal honeycomb pattern</li> <li>• Grainy image</li> <li>• Pagetoid cells in the epidermis</li> <li>• Complex branching dendrites or dendritic cells</li> <li>• Atypical and pleomorphic refractile cells</li> <li>• Presence of bright, highly refractile particles</li> </ul> Morphologic criteria used for nevus diagnosis <ul style="list-style-type: none"> <li>• Normal epidermal architecture with regular honeycomb pattern</li> <li>• Presence of junctional or Ns</li> <li>• Monomorphic refractile cells</li> </ul>
Guitera lentigo maligna score <sup>64</sup>	RCM score ranges from -1 to 7 points Major features (2 points each) <ul style="list-style-type: none"> <li>• Nonedged papillae</li> <li>• Round large pagetoid cells <math>&gt;20 \mu\text{m}</math></li> </ul> Minor features (1 point each) <ul style="list-style-type: none"> <li>• <math>\geq 3</math> cells at the DEJ</li> <li>• Follicular localization of atypical cells</li> <li>• Nucleated cells within the dermal papillae</li> </ul> Minor feature (-1 point) <ul style="list-style-type: none"> <li>• Broadened honeycomb pattern</li> </ul> Score $\geq 2$ suggestive of melanoma diagnosis

BCC, Basal cell carcinoma; C, cobblestone pattern; DEJ, dermoepidermal junction; DF, dermatofibroma; DP, widespread dermal papilla; N, dermal nest; P, pagetoid infiltration; RCM, reflectance confocal microscopy; SK, seborrheic keratosis.

melanoma). Table VIII provides a summary of key RCM findings.

Though melanoma subtypes share many similar RCM features, there are nuances that should be noted. RCM features of melanoma arising on chronically sun-damaged skin (lentigo maligna and lentigo maligna melanoma) characteristically display sheets of atypical melanocytes, mostly with a dendritic shape, in the basal epidermis, surrounding and extending down adnexal openings (Fig 10).<sup>54,56</sup> Nodular melanoma characteristically displays cerebriform dermal nests, but shows less remarkable changes in the epidermis, lacking the density of pagetoid melanocytes and the disarranged epidermal pattern observed in other melanoma subtypes.<sup>57</sup> The scarcity of epidermal criteria may present a pitfall in the RCM diagnosis of nodular melanoma.<sup>58,59</sup> Amelanotic melanoma poses a particular clinical and dermoscopic challenge. With RCM, it shares features with other melanomas; however given the lack of melanin, “hyporeflective pagetoid cells” can be a clue to this diagnosis observed in 85% of cases.<sup>60</sup>

Multiple scoring algorithms exist for the diagnosis of melanoma with RCM. Some involve a decision tree<sup>61</sup> while others involve point assignment for each criterion with subsequent addition for final score attainment.<sup>42,51,62-64</sup> Table IX summarizes these algorithms. In a Cochrane review, pooling sensitivities and specificities across several studies found that the RCM algorithm used by Pellacani has 80% to 100% sensitivity and 67% to 95% specificity.<sup>65</sup> The Segura 2-step algorithm has a sensitivity of 86.1% and specificity of 95.3%, when setting the threshold for melanoma diagnosis to a score  $\geq 0$ .<sup>63</sup> Decreasing the threshold to  $-1$  increased the sensitivity to 100% but decreased the specificity significantly to 57%.<sup>63</sup> The criteria of analysis per Langley et al<sup>66</sup> found a sensitivity of 97% and specificity of 83%.<sup>66</sup> When setting a threshold score of  $\geq 2$  in the Guitera lentigo maligna score, a sensitivity of 85% and specificity of 76% was achieved.<sup>64</sup>

The second article in this continuing medical education series reviewed the main RCM features of cutaneous neoplasms—both malignant and benign. We have provided both dermoscopic and histopathologic correlates to aid in the understanding of RCM findings and to further increase the scope of RCM’s potential alongside other tools at our disposal.

## REFERENCES

1. Argenziano G, Soyer HP, Chimenti S, et al. Dermoscopy of pigmented skin lesions: results of a consensus meeting via the internet. *J Am Acad Dermatol*. 2003;48:679-693.

2. Langley RGB, Burton E, Walsh N, Propperova I, Murray SJ. In vivo confocal scanning laser microscopy of benign lentiginosities: comparison to conventional histology and in vivo characteristics of lentigo maligna. *J Am Acad Dermatol*. 2006; 55:88-97.
3. Pollefliet C, Corstjens H, González S, Hellemans L, Declercq L, Yarosh D. Morphological characterization of solar lentiginosities by in vivo reflectance confocal microscopy: a longitudinal approach. *Int J Cosmet Sci*. 2013;35:149-155.
4. Sanchez VP, Gill M, Gonzalez S. Lentigo. In: González S, Ahlgrimm-Siess V, eds. *Reflectance Confocal Microscopy in Dermatology: Fundamentals and Clinical Applications*. Madrid, Spain: Grupo Aula Médica; 2012:31-34.
5. Ahlgrimm-Siess V, Langley RGB, Hofmann-Wellenhof R. Solar lentigo, seborrheic keratosis and lichen planus-like keratosis. In: Hofmann-Wellenhof R, Pellacani G, Malvehy J, Soyer HP, eds. *Reflectance Confocal Microscopy for Skin Diseases*. 1st ed. New York: Springer; 2012:259-273.
6. Braun RP, Rabinovitz H, Krischer J, et al. Dermoscopy of pigmented seborrheic keratosis. *Arch Dermatol*. 2002;138: 1556-1560.
7. Pezzini C, Mandel VD, Persechino F, et al. Seborrheic keratoses mimicking melanoma unveiled by in vivo reflectance confocal microscopy. *Ski Res Technol*. 2018;24:285-293.
8. Carrera C, Segura S, Aguilera P, et al. Dermoscopy improves the diagnostic accuracy of melanomas clinically resembling seborrheic keratosis: cross-sectional study of the ability to detect seborrheic keratosis-like melanomas by a group of dermatologists with varying degrees of experience. *Dermatology*. 2018;233:471-479.
9. Tavoloni Braga JC, Scope A, Klaz I, Mecca P, Spencer P, Marghoob AA. Melanoma mimicking seborrheic keratosis: an error of perception precluding correct dermoscopic diagnosis. *J Am Acad Dermatol*. 2008;58:875-880.
10. Braga JCT, Scope A, Klaz I, et al. The significance of reflectance confocal microscopy in the assessment of solitary pink skin lesions. *J Am Acad Dermatol*. 2009;61:230-241.
11. Ahlgrimm-Siess V, Cao T, Oliviero M, et al. Seborrheic keratosis: reflectance confocal microscopy features and correlation with dermoscopy. *J Am Acad Dermatol*. 2013; 69:120-126.
12. Kopf AW, Rabinovitz H, Marghoob A, et al. “Fat fingers”: a clue in the dermoscopic diagnosis of seborrheic keratoses. *J Am Acad Dermatol*. 2006;55:1089-1091.
13. González S. *Reflectance Confocal Microscopy of Cutaneous Tumors*. 2nd ed. Boca Raton, FL: CRC Press; 2017.
14. Bassoli S, Rabinovitz HS, Pellacani G, et al. Reflectance confocal microscopy criteria of lichen planus-like keratosis. *J Eur Acad Dermatol Venereol*. 2012;26:578-590.
15. Shapiro L, Ackerman AB. Solitary lichen planus-like keratosis. *Dermatology*. 1966;132:386-392.
16. Goette DK. Benign lichenoid keratosis. *Arch Dermatol*. 1980; 116:780-782.
17. Zaballos P, Ara M, Puig S, Malvehy J. Dermoscopy of sebaceous hyperplasia. *Arch Dermatol*. 2005;141:808.
18. Bryden AM, Dawe RS, Fleming C. Dermatoscopic features of benign sebaceous proliferation. *Clin Exp Dermatol*. 2004;29: 676-677.
19. Salerni G, Lovato L, Puig S, Malvehy J. Sebaceous hyperplasia. In: González S, Ahlgrimm-Siess V, eds. *Reflectance Confocal Microscopy in Dermatology: Fundamentals and Clinical Applications*. Madrid, Spain: Grupo Aula Médica; 2012:89-90.
20. Shahriari N, Grant-Kels JM, Rabinovitz H, Oliviero M, Scope A. In vivo reflectance confocal microscopy image interpretation for the dermatopathologist. *J Cutan Pathol*. 2018;45:187-197.

21. Aghassi D, González E, Anderson RR, Rajadhyaksha M, González S. Elucidating the pulsed-dye laser treatment of sebaceous hyperplasia in vivo with real-time confocal scanning laser microscopy. *J Am Acad Dermatol*. 2000;43:49-53.
22. Propperova I, Langley RGB. Reflectance-mode confocal microscopy for the diagnosis of sebaceous hyperplasia in vivo. *Arch Dermatol*. 2007;143:134.
23. González S, White WM, Rajadhyaksha M, Anderson RR, González E. Confocal imaging of sebaceous gland hyperplasia in vivo to assess efficacy and mechanism of pulsed dye laser treatment. *Lasers Surg Med*. 1999;25:8-12.
24. Casson P. Basal cell carcinoma. *Clin Plast Surg*. 1980;7:301-311.
25. González S, Tannous Z. Real-time, in vivo confocal reflectance microscopy of basal cell carcinoma. *J Am Acad Dermatol*. 2002;47:869-874.
26. Sanchez VP, Fernandez M, Gill MGS. Basal cell carcinoma. In: González S, Ahlgrimm-Siess V, eds. *Reflectance Confocal Microscopy in Dermatology: Fundamentals and Clinical Applications*. Madrid, Spain: Grupo Aula Médica; 2012:77-80.
27. Segura S, Puig S, Carrera C, Palou J, Malvey J. Dendritic cells in pigmented basal cell carcinoma. *Arch Dermatol*. 2007;143:883-886.
28. Rabinovitz H, Oliviero M, Malvey J, Puig S. Dermoscopic and histopathologic correlations. In: Hofmann-Wellenhof R, Pellacani G, Malvey J, Soyer HP, eds. *Reflectance Confocal Microscopy for Skin Diseases*. New York: Springer; 2012:253. First.
29. Ahlgrimm-siess V, Rabinovitz HS, Oliviero M, Hofmann-wellenhof R, Marghoob AA, Scope A. Confocal microscopy in skin cancer. In: Rigel D, ed. *Cancer of the Skin*. Elsevier; 2011:407-472.
30. Aghassi D, Anderson RR, González S. Confocal laser microscopic imaging of actinic keratoses in vivo: a preliminary report. *J Am Acad Dermatol*. 2000;43:42-48.
31. Ulrich M, Maltusch A, Röwert-Huber J, et al. Actinic keratoses: non-invasive diagnosis for field cancerisation. *Br J Dermatol*. 2007;156(suppl 3):13-17.
32. Astner S, Gonzalez S, Ulrich M. Actinic keratosis. In: Gonzalez S, Ahlgrimm-Siess V, eds. *Reflectance Confocal Microscopy in Dermatology: Fundamentals and Clinical Applications*. Madrid, Spain: Grupo Aula Medica; 2012:69-71.
33. Tan JM, Lambie D, Sinnya S, et al. Histopathology and reflectance confocal microscopy features of photodamaged skin and actinic keratosis. *J Eur Acad Dermatol Venereol*. 2016;30:1901-1911.
34. Rishpon A, Kim N, Scope A, et al. Reflectance confocal microscopy criteria for squamous cell carcinomas and actinic keratoses. *Arch Dermatol*. 2009;145:766-772.
35. González S, Sánchez V, González-Rodríguez A, Parrado C, Ullrich M. Confocal microscopy patterns in nonmelanoma skin cancer and clinical applications. *Actas Dermosifiliogr*. 2014;105:446-458.
36. Que S, Fraga-Braghiroli N, Grant-Kels J, Rabinovitz H, Oliviero M, Scope A. A pink papule on the back of an 82-year-old man: an example of the buttonhole sign on reflectance confocal microscopy. *Dermatol Pract Concept*. 2016;6:1-2.
37. Manfredini M, Longo C, Ferrari B, et al. Dermoscopic and reflectance confocal microscopy features of cutaneous squamous cell carcinoma. *J Eur Acad Dermatol Venereol*. 2017;31:1828-1833.
38. Shahriari N, Grant-Kels JM, Rabinovitz HS, Oliviero M, Scope A. Reflectance confocal microscopy criteria of pigmented squamous cell carcinoma in situ. *Am J Dermatopathol*. 2018;40:173-179.
39. Lovato L, Salerni G, Carrera C, Puig S, Malvey J. Acquired common and congenital melanocytic nevi. In: González S, Ahlgrimm-Siess V, eds. *Reflectance Confocal Microscopy in Dermatology: Fundamentals and Clinical Applications*. Madrid, Spain: Grupo Aula Médica; 2012:35-37.
40. Bassoli S, Ahlgrimm-Siess V, Casari A, Pellacani G. Common nevi. In: Hofmann-Wellenhof R, Pellacani G, eds. *Reflectance Confocal Microscopy for Skin Diseases*. London: Springer; 2012:73-86.
41. Pellacani G, Scope A, Farnetani F, et al. Towards an in vivo morphologic classification of melanocytic nevi. *J Eur Acad Dermatol Venereol*. 2014;28:864-872.
42. Pellacani G, Cesinaro AM, Seidenari S. Reflectance-mode confocal microscopy of pigmented skin lesions-improvement in melanoma diagnostic specificity. *J Am Acad Dermatol*. 2005;53:979-985.
43. Langley RGB, Rajadhyaksha M, Dwyer PJ, Sober AJ, Flotte TJ, Anderson RR. Confocal scanning laser microscopy of benign and malignant melanocytic skin lesions in vivo. *J Am Acad Dermatol*. 2001;45:365-376.
44. Gerger A, Koller S, Kern T, et al. Diagnostic applicability of in vivo confocal laser scanning microscopy in melanocytic skin tumors. *J Invest Dermatol*. 2005;124:493-498.
45. Que SKT, Fraga-Braghiroli N, Grant-Kels JM, Rabinovitz HS, Oliviero M, Scope A. Through the looking glass: basics and principles of reflectance confocal microscopy. *J Am Acad Dermatol*. 2015;73:276-284.
46. Pellacani G, Scope A, Ferrari B, et al. New insights into nevogenesis: in vivo characterization and follow-up of melanocytic nevi by reflectance confocal microscopy. *J Am Acad Dermatol*. 2009;61:1001-1013.
47. Salerni G, Lovato L, Malvey J, Puig S. Dysplastic nevi. In: González S, Ahlgrimm-Siess V, eds. *Reflectance Confocal Microscopy in Dermatology: Fundamentals and Clinical Applications*. Madrid, Spain: Grupo Aula Médica; 2012:43-45.
48. Pellacani G, Farnetani F, Gonzalez S, et al. In vivo confocal microscopy for detection and grading of dysplastic nevi: a pilot study. *J Am Acad Dermatol*. 2012;66:e109-e121.
49. Pellacani G, Farnetani F, Argenziano G, Zalaudek I, Longo CMG. Atypical/dysplastic nevi. In: Hofmann-Wellenhof R, Pellacani G, Malvey J, Soyer HP, eds. *Reflectance Confocal Microscopy for Skin Diseases*. London: Springer; 2012:87-89.
50. Pellacani G, Cesinaro AM, Seidenari S. Reflectance-mode confocal microscopy for the in vivo characterization of pagetoid melanocytosis in melanomas and nevi. *J Invest Dermatol*. 2005;53:979-985.
51. Pellacani G, Cesinaro AM, Longo C, Grana C, Seidenari S. Microscopic in vivo description of cellular architecture of dermoscopic pigment network in nevi and melanomas. *Arch Dermatol*. 2005;141:147-154.
52. Pellacani G, Longo C, Ferrara G, et al. Spitz nevi: in vivo confocal microscopic features, dermatoscopic aspects, histopathologic correlates, and diagnostic significance. *J Am Acad Dermatol*. 2009;124:493-498.
53. Pellacani G, Longo C, Pupelli G, et al. Spitz/Reed nevus. In: González S, Ahlgrimm-Siess V, eds. *Reflectance Confocal Microscopy in Dermatology: Fundamentals and Clinical Applications*. Madrid, Spain: Grupo Aula Médica; 2012:39-41.
54. Pellacani G, Scope A, Gonzalez S, et al. Reflectance confocal microscopy made easy: the 4 must-know key features for the diagnosis of melanoma and nonmelanoma skin cancers. *J Am Acad Dermatol*. 2019;81:520-526.
55. Pupelli G, Veneziano L, Longo C, Rezze GG, Soyer HP, Pellacani G. Melanocytic lesions: dermoscopic and

- histopathologic correlations. In: Hofmann-Wellenhof R, Pellacani G, Malvehy J, Soyer HP, eds. *Reflectance Confocal Microscopy for Skin Diseases*. Heidelberg, Germany: Springer-Verlag; 2012:59.
56. Ahlgrim-Siess V, Massone C, Scope A, et al. Reflectance confocal microscopy of facial lentigo maligna and lentigo maligna melanoma: a preliminary study. *Br J Dermatol*. 2009;161:1307-1316.
  57. Segura S, Pellacani G, Puig S, et al. In vivo microscopic features of nodular melanomas: dermoscopy, confocal microscopy, and histopathologic correlates. *Arch Dermatol*. 2008;144:1311-1320.
  58. Coco V, Farnetani F, Cesinaro AM, et al. False-negative cases on confocal microscopy examination: a retrospective evaluation and critical reappraisal. *Dermatology*. 2016;232:189-197.
  59. Longo C, Farnetani F, Ciardo S, et al. Is confocal microscopy a valuable tool in diagnosing nodular lesions? A study of 140 cases. *Br J Dermatol*. 2013;169:58-67.
  60. Losi A, Longo C, Cesinaro AM, et al. Hyporeflective pagetoid cells: a new clue for amelanotic melanoma diagnosis by reflectance confocal microscopy. *Br J Dermatol*. 2014;171:48-54.
  61. Gerger A, Wiltgen M, Langsenlehner U, et al. Diagnostic image analysis of malignant melanoma in in vivo confocal laser-scanning microscopy: a preliminary study. *Ski Res Technol*. 2008;14:359-363.
  62. Guitera P, Menzies SW, Longo C, Cesinaro AM, Scolyer RA, Pellacani G. In vivo confocal microscopy for diagnosis of melanoma and basal cell carcinoma using a two-step method: analysis of 710 consecutive clinically equivocal cases. *J Invest Dermatol*. 2012;132:2386-2394.
  63. Segura S, Puig S, Carrera C, Palou J, Malvehy J. Development of a two-step method for the diagnosis of melanoma by reflectance confocal microscopy. *J Am Acad Dermatol*. 2009;61:216-229.
  64. Guitera P, Pellacani G, Crotty KA, et al. The impact of in vivo reflectance confocal microscopy on the diagnostic accuracy of lentigo maligna and equivocal pigmented and nonpigmented macules of the face. *J Invest Dermatol*. 2010;130:2080-2091.
  65. Dinnes J, Deeks JJ, Saleh D, et al. Reflectance confocal microscopy for diagnosing cutaneous melanoma in adults. *Cochrane Database Syst Rev*. 2018;12:CD013190.
  66. Langley RGB, Walsh N, Sutherland AE, et al. The diagnostic accuracy of in vivo confocal scanning laser microscopy compared to dermoscopy of benign and malignant melanocytic lesions: a prospective study. *Dermatology*. 2007;215:365-372.

---

## Answers to CME examination

Identification No. JB0121

January 2021 issue of the Journal of the American Academy of Dermatology.

Shabriari N, Grant-Kels JM, Rabinovitz H, Oliviero M, Scope A. *J Am Acad Dermatol* 2021;84:17-31.

1. b
2. c

3. b